Theor Chem Acc (2011) 128:593–599
DOI 10.1007/s00214-010-0802-y

REGULAR ARTICLE

A molecular mechanism for direct generation of nitric oxide, peroxynitrite and superoxide in the reaction of nitroglycerin with a cysteil-cysteine derivative

Juan Soto · Francisco J. Avila · Juan C. Otero · Daniel Peláez · Juan F. Arenas

Received: 17 June 2010 / Accepted: 18 August 2010 / Published online: 5 September 2010

Abstract The molecular mechanism of the reaction of nitroglycerin with a cysteil-cysteine derivative has been studied by quantum mechanical methods; in particular, density functional theory with the accurate meta exchange-correlation functional M06-2X was used. The first reaction step is nitration of a deprotonated cysteine of the dipeptide. Afterward, six reaction steps are followed to yield the final products of the process: 1,2-glyceryl dinitrate (GDN), nitric oxide (NO), peroxynitrite anion ($^{-}$OONO), and superoxide anion (O_2^{-}) plus an intramolecular disulfide bond in the dipeptide. Two nitroglycerin molecules are decomposed for each disulfide bond formation in the dipeptide. A reducing agent is necessary to complete the global reaction. The action of the reductant triggers S-peroxynitrite formation, which, in turn, can decompose into $^{-}$OONO or NO plus O_2^{-}.

Keywords Nitroglycerin · Aldehyde dehydrogenase · Molecular mechanism · Quantum chemistry

1 Introduction

Nitroglycerin (GTN), synthesized by Ascanio Sobrero in 1847 and origin of Alfred Nobel's myth, has been used in Medicine almost since its discovery [1, 2]. Constantin Hering used it for the first time as a homeopathic remedy for headache in 1849 [1]. However, the relevant medical application of GTN lies in its potent vasodilating action. It has been applied clinically since the late nineteenth century for the treatment of coronary artery disease (angina pectoris), congestive heart failure and myocardial infarction [3]. Although the first reported application of GTN for angina pectoris relief is due to William Murrell in 1879 [4], it seems that the antianginal effect of GTN was discovered in Nobel's dynamite factories in the late 1860s [2]. Significant progress toward understanding of the GTN mode of action did not arrive until the end of the twentieth century [1], thanks to the work of several research groups [5–10] that claimed to identify nitric oxide (NO) generated from GTN and other nitro-compounds as the species responsible for the vasodilating action of such drugs. However, the GTN/NO hypothesis has been questioned, and recent studies have concluded that GTN induces vasorelaxation without intermediacy of the free radical nitric oxide [11–13]. Another key step in the knowledge of the biotransformation of GTN took place in 2002 when Chen et al. [14] demonstrated that mitochondrial aldehyde dehydrogenase (mtALDH) was an essential enzyme in the biodegradation of clinical levels of GTN [14, 15]. The active site of the protein is the cysteine residue 302 (Cys302), which is adjacent to and flanked by other two cysteine residues (Cys301 and Cys303). In support of the relevancy of mitochondrial aldehyde dehydrogenase in the enzymatic biotransformation of GTN, it must be also noted that such an enzyme plays also a significant role in the development of GTN tolerance [15–17]. Nitrate tolerance is an important issue related to medical administration of GTN, that is, the reduction of the effect of the drug or the requirement of higher doses that appears after continuous

Published as part of the special issue celebrating theoretic and computational chemistry in Spain.

Electronic supplementary material The online version of this article (doi:10.1007/s00214-010-0802-y) contains supplementary material, which is available to authorized users.

J. Soto (✉) · F. J. Avila · J. C. Otero · D. Peláez · J. F. Arenas
Department of Physical Chemistry,
Faculty of Science, University of Málaga,
Campus de Teatinos, 29071 Málaga, Spain
e-mail: soto@uma.ess

application of GTN [1, 2]. The chemical basis of this effect is not yet known; a hypothesis assigns the nitrate tolerance phenomenon to the increased bioavailability of superoxide anion (O_2^-) [18–21], which decreases the activity of endothelial nitric oxide synthase [20]. Some authors have suggested that superoxide is released directly from GTN after its administration [22–24]. Importantly, peroxynitrite ($^-$OONO) is another relevant species involved in the tolerance mechanism [21, 25]. It could be formed by the interaction between O_2^- and NO, two direct products of biodegradation of GTN [21].

Despite the important achievements reached in the knowledge of biodegradation of GTN, the precise molecular mechanism, by which nitroglycerin decomposes, remains elusive [2, 3, 11, 26, 27]. Moreover, as Ignarro wrote, by understanding the molecular mechanism of nitroglycerin bioactivation, it would be possible to design and develop novel nitrovasodilator drugs that do not cause tolerance [2]. In particular, the mechanism of ALDH-catalyzed GTN denitration is not known [3]. It is accepted [3] that the initial step of the reaction is nucleophilic attack by GTN to Cys302, leading to formation of a thionitrate intermediate and release of the 1,2-glyceryl dinitrate (1,1-GDN) [16]. The reaction advances to generate nitrite with the most remarkable characteristic that formation of 1,2-GDN and nitrite is stoichiometric. Nitrite formation indicates that the thionitrate intermediate is reduced and not hydrolyzed. Therefore, oxidation and inactivation of the protein may involve formation of a disulfide bond that involves the active site Cys302 [16].

Therefore, by assuming that ALDH is an important enzyme involved in the biochemistry of nitroglycerin, the main purpose of this work is to rationalize the reaction paths involved in the chemistry of nitroglycerin with the active site of the enzyme Cys302–Cys301/303. For such an objective, we will make use of quantum chemical methods based on density functional theory. As a structural model of the protein active site, we have chosen the dipeptide consisting of two cysteine residues, whose initial arrangement corresponds to the protein fragment Cys302–Cys303 of human liver mitochondrial aldehyde dehydrogenase (Fig. 1). The three-dimensional structure of this protein was determined by Ni et al. [28] with X-ray diffraction (PDB code: 1CW3, resolution = 2.58 Å). The structure of the fragment of the protein chosen as model has been fully optimized without geometrical constraints starting at the experimental geometry. It is remarkable that the calculation converges to an optimized structure that does not significantly differ from the initial geometry, excepting the bonds in which protons are involved as it was expected. Interestingly, the optimization process converges monotonically to a minimum, which indicates that the model structure is more rigid than it would be expected from a visual inspection. With the selected

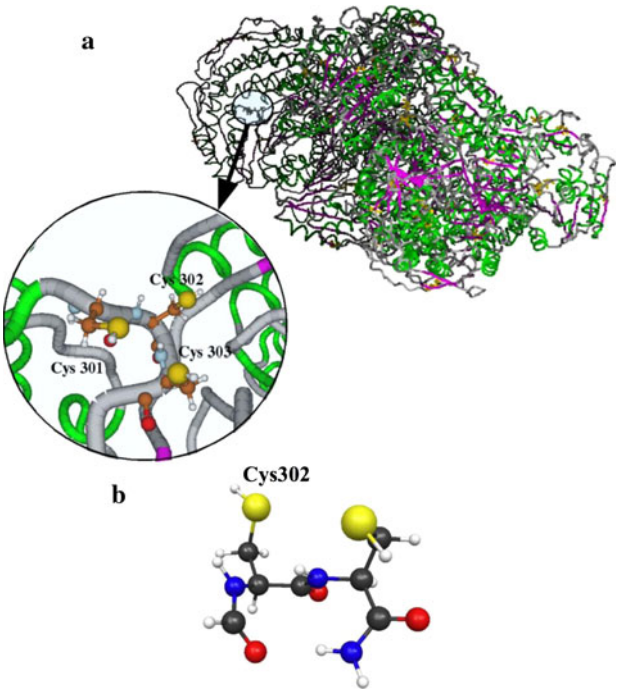

Fig. 1 **a** Structure of human liver mithocondrial aldehyde dehydrogenase (PDB code: 1CW3) crystallized and resolved by X-ray diffraction. **b** Optimized structure of the dipeptide used as molecular model for its reaction with nitroglycerin

model, it will be demonstrated how nitric oxide, peroxynitrite, and superoxide can be directly generated in the reaction of GTN with the dipeptide. Extrapolation of our results to the complete enzyme must be done with extreme caution, provided that the surrounding fragments of the enzyme would affect the calculated energy barriers, as well as affecting stability of different conformations of the reaction center.

2 Computational details

To obtain insight into the mechanism of nitroglycerin bioactivation, we have applied density functional theory with the meta exchange–correlation functional M06-2X [29], in conjunction with the 6-31+G(d,p) basis set [30]. This functional is suitable for applications involving main-group thermochemistry and kinetics; interestingly, it can properly describe noncovalent interactions. Each stationary point on the potential energy surface has been characterized by its analytically computed harmonic frequencies. For each transition state (1 imaginary frequency), an intrinsic reaction coordinate (IRC) [31] calculation has been performed as well. Therefore, the products and reactants connected by the respective transition states have been unambiguously localized by means of such IRC calculations. Localization of minima and transition states has been carried out with a starting set of Cartesian

coordinates. Partial electric charges on atoms have been determined with the atomic polar tensor method [32]. All of the electronic structure calculations have been done with the program GAUSSIAN09 [33]. Gibbs activation energies and dissociation energies have been calculated with the expressions given by statistical thermodynamics and transition state theory with a program written by ourselves. Molecular structures have been analyzed with the aid of MacMolPlt [34] and MOLDEN [35] programs.

3 Results and discussion

The mechanism for the reaction of nitroglycerin with the derivative of cysteil-cysteine is given in Fig. 2. A detailed discussion of every reaction step involved in the biodegradation of GTN will be given in the next subsections. We represent schematically the dipeptide by HS_α–E–$S_\beta H$, where HS_α denotes the Cys302 residue and $S_\beta H$ the Cys301/303 residue. The first step of the reaction is nitration of dipeptide by attack of GTN at the deprotonated sulfur of cysteine yielding a neutral thionitrate (O_2N–S_α–E–$S_\beta H$) plus the corresponding alcoxide of nitroglycerin ($^-OCH_2$–$CHONO_2$–CH_2ONO_2); second, one of the cysteine residues Cys301/303, which are adjacent to Cys302, is deprotonated (O_2N–S_α–E–S_β^-); third, the nitro moiety linked to Cys302 migrates to deprotonated Cys301/303, yielding the sulfenyl nitrite complex ($^-S_\alpha$–E–$S_\beta ONO$); fourth, NO elimination from the nitrite generated in the preceding step generates an anion radical intermediate

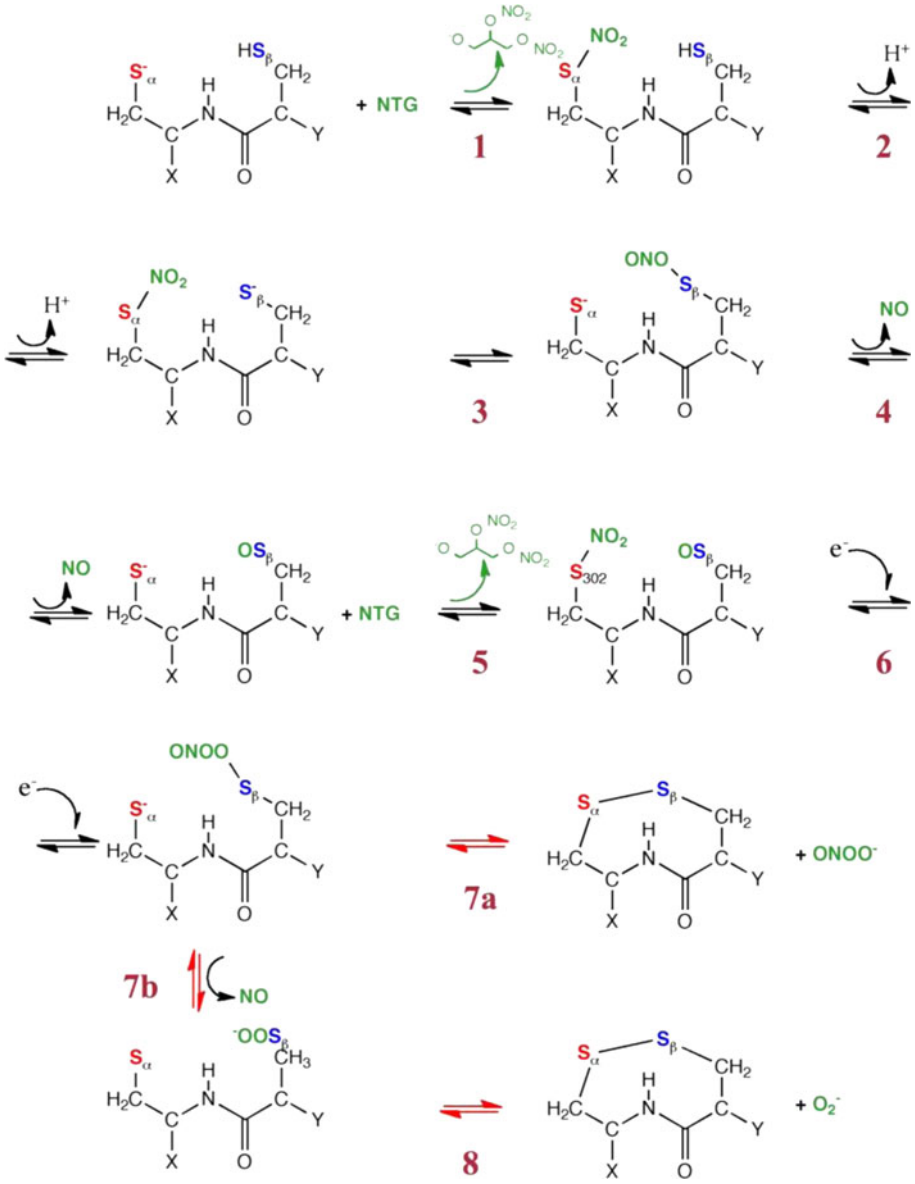

Fig. 2 Molecular mechanism for the reaction of nitroglycerin with a cysteil-cysteine derivative. (*1*) first nitration; (*2*) deprotonation of Cys301/303; (*3*) ONO migration; (*4*) NO elimination; (*5*) second nitration; (*6*) concerted electron acceptation and ONO migration; (*7a*) peroxinitrate anion release and disulfide bond formation; (*7b*) NO elimination; (*8*) superoxide anion release and disulfide bond formation. S_α residue 302; S_β residue or 303. **X**: $–CONH_2$; **Y**: –NHCHO

Table 1 Energetic (kcal/mol) of the elemental steps involved in the reaction of nitroglycerin with a cysteil-cisteine derivative

Step	Reaction	$\Delta_a U(0)$[a]	$\Delta_a G^{\circ,b}$
1	$^{-}S_{\alpha}$–E–S_{β}H—GTN → O_2N–S_{α}–E–S_{β}H + $^{-}$GDN	20.9	20.2
1b	HS_{α}–E–S_{β}H—GTN → O_2N–S_{α}–E–S_{β}H + GDN	43.4	46.3
3a	O_2N–S_{α}–E–S_{β}^{-} → $^{-}S_{\alpha}$–E–S_{β}ONO	23.2	24.4
3b	O_2N–S_{α}–E–S_{β}^{-} → E–S_2 + NO_2^{-}	29.1	29.4
3c	O_2N–S_{α}–E–$S_{\beta\beta}$H → ONO–S_{α}–E–S_{β}H	54.0	54.1
4	$^{-}S_{\alpha}$–E–S_{β}ONO + → $^{-}S_{\alpha}$–E–S_{β}O + NO	5.9	−3.7[c]
5	$^{-}S_{\alpha}$–E–S_{β}O—GTN → O_2N–S_{α}–E–S_{β}O + $^{-}$GDN	6.2	7.2
6	O_2N–S_{α}–E–S_{β}O + 1e^{-}→O_2N–S_{α}–E–$S_{\beta}O^{-}$→S_{α}–E–S_{β}OONO^{-}	59.9[d]	
7a	S_{α}–E–S_{β}OONO^{-} → E–S_2 + $^{-}$OONO	19.3	9.4[c]
7b	S_{α}–E–S_{β}OONO^{-} → S_{α}–E–$S_{\beta}O^{-}$ + NO	23.0	14.8[c]
8b	S_{α}–E–$S_{\beta}O^{-}$ → E–S_2 + O_2^{-}	25.0	17.8[c]

All reactions taken as unimolecular

[a] Internal activation energy at 0 K calculated as the energy difference between the ground vibrational levels of the reactive species and its corresponding transition state or final products

[b] Standard Gibbs activation energy

[c] Standard Gibbs dissociation energy

[d] Adiabatic electron affinity calculated as the energy difference between the ground vibrational level of the anion and the ground vibrational level of the neutral molecule

($[S_{\alpha}$–E–$S_{\beta}O^{\cdot}]^{-}$); fifth, second nitration on Cys302 gives a thionitrate neutral radical, (O_2N–S_{α}–E–S_{β}O); sixth, a reductant transfers one electron to O_2N–S_{α}–E–S_{β}O and triggers migration of the NO_2 moiety to Cys301/303 forming a peroxynitrite complex ($[S_{\alpha}$–E–S_{β}OONO$]^{-}$); seventh, release of $OONO^{-}$ (Step 7a) or NO (Step 7b) from $[S_{\alpha}$–E–S_{β}OONO$]^{-}$; eighth, if elimination of nitric oxide takes place (7b), the anionic S-peroxythiol $[S_{\alpha}$–E–S_{β}OO$]^{-}$ can easily liberate superoxide anion forming an intramolecular disulfide bond. The energetic of all the steps involved in the global mechanism is given in Table 1. The molecular structures of all the species (reactants, products, intermediates, and transition states) involved in this reaction and the intrinsic reaction coordinates are reported in the supplementary material.

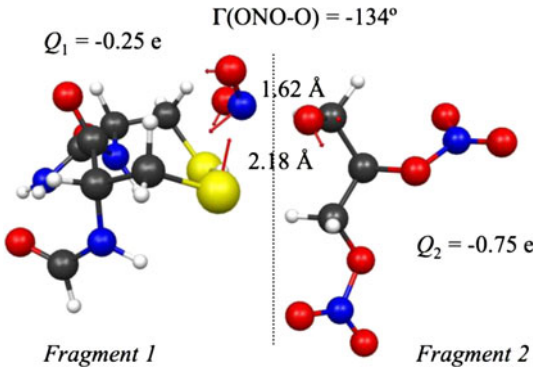

Fig. 3 Molecular geometry of the transition state for first nitration of the dipeptide. The *arrows* represent the direction of the transition vector. *Q* represents the charge of each reaction fragment at the transition state geometry

3.1 First nitration (1)

The initial reaction step is denitration of nitroglycerin to yield deprotonated 1,2-glyceryl dinitrate plus nitrated dipeptide (O_2N–S_{α}–E–S_{β}H). This step takes place when GTN attacks at the deprotonated sulfur of Cys302. The Gibbs activation energy of the process is rather low ($\Delta_a G^{\circ}$ = 20.2 kcal/mol). It is remarkable the arrangement of the nitro group in the molecular structure of the transition state of this reaction, which is highly pyramidalized (Fig. 3) like the geometries of the radical anions of other nitro-compounds [36]. In fact, the calculations indicate that charge transfer already occurs at the transition state conformation, that is, charge on the salient fragment ($^{-}OCH_2$–$CHONO_2$–CH_2ONO_2) is close to −1. The nitration reaction on protonated sulfur of Cys302 has also been investigated. We have been able to find the minimum energy path for this step (Step 1b); however, the resultant Gibbs activation energy is very high ($\Delta_a G^{\circ}$ = 46.3 kcal/mol) and it must not be considered as a catalyzed reaction (Table 1). As a consequence, it seems a reasonable hypothesis that the initial reaction takes place on deprotonated sulfur of Cys302, which is in accordance with the optimum pH (∼9) for denitration activity of the enzyme [14, 16], and with other reaction schemes proposed in the literature [3].

3.2 Sulfenyl nitrite formation and NO extrusion (2–4)

After nitration of the dipeptide and deprotonation of Cys301/303 (Step 2), two reaction paths are available: (1) sulfenyl nitrite formation, that is, the NO_2 moiety linked to Cys302 migrates to Cys301/303 (Step 3a) to yield sulfenyl nitrite ($^{-}S_{\alpha}$–E–S_{β}ONO); (2) denitration concurrent with intramolecular disulfide bond formation (Step 3b). Sulfenyl nitrite formation ($\Delta_a G° = 24.3$ kcal/mol) is favored against denitration ($\Delta_a G° = 29.1$ kcal/mol). If sulfenyl nitrite is formed ($^{-}S_{\alpha}$–E–S_{β}ONO), elimination of nitric oxide to give the corresponding radical anion ($^{-}S_{\alpha}$–E–S_{β}O, Step 4) is a spontaneous process provided that it has negative Gibbs dissociation energy ($\Delta_d G° = -3.7$ kcal/mol). To finish this section, it must be noted that it was possible to find the path for the rearrangement of the nitro moiety to give the nitrite on Cys302 when the other cysteine residue was protonated (O_2N–S_{α}–E–S_{β}H → ONO–S_{α}–E–S_{β}H). This is a theoretically well-studied reaction for many other nitro-compounds [36–42]. However, this process must be discarded for the system under consideration because of its prohibitive high activation energy ($\Delta_a G° = 54.1$ kcal/mol, Table 1).

3.3 Second nitration (5)

The radical anion formed in the previous step ($^{-}S_{\alpha}$–E–S_{β}O) has partial negative charge ($Q = -0.8$ *e*) on the sulfur atom of Cys302 and can suffer a second nitration to give a neutral intermediate (O_2N–S_{α}–E–S_{β}O, Step 5). The Gibbs activation energy of this process is considerably lower than that of the first nitration ($\Delta_a G° = 7.2$ kcal/mol).

3.4 Reduction of the neutral intermediate and S-peroxynitrite formation (6)

Once the second nitration is completed, a reductant transfers an electron to the intermediate just formed to give an anionic complex ($[O_2N$–S_{α}–E–$S_{\beta}O]^{-}$, Step 6). Neutral O_2N–S_{α}–E–S_{β}O has positive adiabatic electron affinity, that is, the energy of the ground vibrational energy level of the negative ion lies below the ground state of the neutral species (EA = 60 kcal/mol). Furthermore, on the potential energy of the anion $[O_2N$–S_{α}–E–$S_{\beta}O]^{-}$, we have found a transition state that connects the minimum of the anion $[O_2N$–S_{α}–E–$S_{\beta}O]^{-}$ with a peroxynitrite complex $[S_{\alpha}$–E–$S_{\beta}OONO]^{-}$ (Step 7). This transition state has two very remarkable features: (1) its molecular structure is close to the geometry of the neutral intermediate (O2N-Sα-E-Sβ O); (2) the ground vibrational energy level of the anionic transition state lies 13 kcal/mol below the ground state of the neutral minimum (Fig. 4). If we assume at this point that electron donation from a reductant takes place at the geometry of the neutral species (vertical electron transference), the corresponding anion is formed in an excited vibrational state. This is in accordance with experiments in electron impact spectroscopy, where it is firmly established that for a neutral species having positive electron affinity, only the higher vibrational states of the negative ion, namely those that lie above the ground state of the neutral molecule, can be reached by electron impact [43]. To our concern, when charge transfer occurs: (1) the molecular structure of the neutral complex is close to the anionic transition state for S-peroxynitrite formation and (2) there is enough energy for generation of S-peroxynitrite. Therefore, the route for S-peroxynitrite formation triggered by a reductive species is accessible.

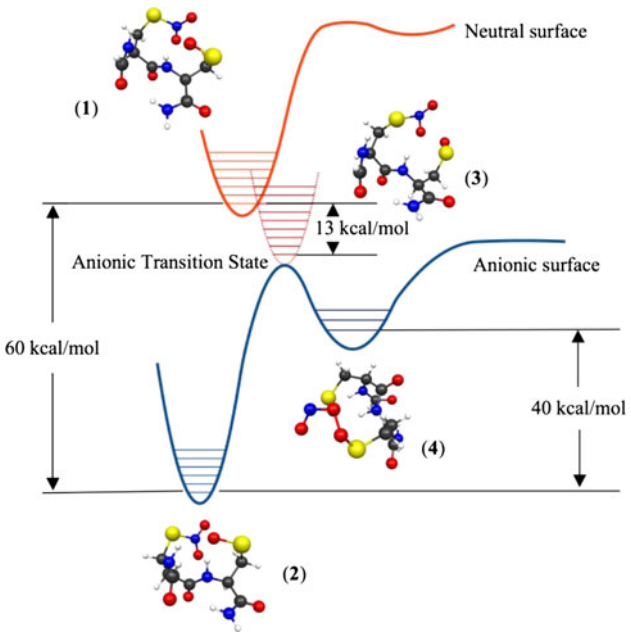

Fig. 4 Schematic representation of the potential energy surfaces (neutral and anionic) involved in S-peroxynitritethiol formation. Geometry of (*1*) neutral minimum; (*2*) anionic minimum; (*3*) anionic transition state leading to S-peroxynitritethiol formation; (*4*) S-peroxynitritethiol

3.5 $^{-}$OONO release (7a)

The S-peroxynitrite complex formed in the preceding step ($^{-}[S_{\alpha}$–E–$S_{\beta}OONO]^{-}$) can release $^{-}$OONO concurrent with formation of an intramolecular disulfide bond. The standard Gibbs dissociation energy of this process is 9.4 kcal/mol (Step 7a). The potential energy surface of this process increases asymptotically from the minimum to dissociation products; in consequence, there is no saddle point on the surface of the reaction channel.

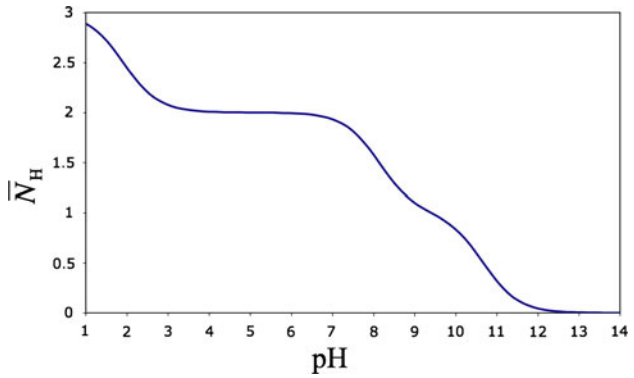

Fig. 5 Proton affinity curve of cysteine

3.6 Nitric Oxide elimination and O_2^- generation (7b and 8)

An alternative path to step 7a is nitric oxide extrusion from the S-peroxynitrite an S-peroxy complex (Step 7b, $[S_\alpha\text{–}E\text{–}S_\beta OO]^-$, $\Delta_d G° = 14.8$ kcal/mol), which, in turn, eliminates superoxide anion and forms an intramolecular disulfide bond (Step 8, $\Delta_d G° = 17.8$ kcal/mol). Like in step 7a, the potential energy surfaces of both processes increase asymptotically from each minimum to the respective dissociation products.

4 Concluding remarks

It is beyond the scope of this work to establish the enzyme that catalyzes the decomposition of nitroglycerin. We have reported a reaction mechanism for the degradation of nitroglycerin when it reacts with a derivative of the cysteil-cysteine dipeptide. It is proposed a mechanism for direct formation of nitric oxide, superoxide, and peroxynitrite, three chemical species related to vasodilating and tolerance effects of nitroglycerin can be generated directly from the reaction of GTN with the dipeptide. Direct comparison of our results with experimental kinetic measurements must be done with extreme caution. For example, reaction **1** must not be compared with the reaction of GTN with cysteine (or cysteine derivatives) in solution; the proper comparison must be done with reaction **1b**. It is experimentally found that GTN reacts slowly at pH 7.4 with cysteine and other organic thiols to give disulfide, inorganic nitrite, and the two corresponding glyceryl dinitrates as products [24, 44, 45]. However, the proton-binding curve of cysteine shows that cysteine does not form thiolate at neutral pH, since its sulfur atom is protonated (the estimated average number [46] $\bar{N}_H$ of acidic protons per cysteine residue is 1.9 at pH 7.4 (Fig. 5); acid dissociation constants are taken from Ref. [47]).

Acknowledgments This research has been supported by the Spanish MICINN (Project Numbers CTQ2009-08549 and CTQ2006-02330) and Junta de Andalucia (Project Number FQM-01895). FA thanks Junta de Andalucía for the Grant P06-FQM-01895. The authors thank as well the SCAI of the University of Málaga for computational facilities and D. Rafael Larrosa for technical support.

References

1. Marsh N, Marsh A (2000) Clin Exp Pharmacol Physiol 27:313–319
2. Ignarro LJ (2002) Proc Natl Acad Sci USA 99:7816–7817
3. Mayer B, Beretta M, Brit J (2008) Pharmacol 155:170–184
4. Murrell W (1879) Lancet 113:80–81
5. Arnold WP, Mittal CK, Katsuki S, Murad F (1977) Proc Natl Acad Sci USA 74:3203–3207
6. Furchgott RF, Zawadzki JV (1980) Nature 288:373–376
7. Murad F, Arnold WP, Mittal CK, Braughler JM (1979) Adv Cycl Nucl Prot Phosphoryl Res 11:175–204
8. Cherry PD, Furchgott RF, Zawadzki JV, Jothianandan D (1982) Proc Natl Acad Sci USA 72:2106–2110
9. Ignarro LJ, Buga GM, Wood KS, Byrns RE, Chaudhury G (1987) Proc Natl Acad Sci USA 84:9265–9269
10. Palmer RMJ, Ferrige AG, Moncada S (1987) Nature 327:524–526
11. Millar MR, Wadsworth RM (2009) Br J Pharmacol 157:565–567
12. Kleschyov AL, Oelze M, Daiber A, Huang Y, Mollnau H, Schulz E, Sydow K, Fichtlscherer B, Mülsch A, Münzel T (2003) Circ Res 93:e104–e112
13. Núñez C, Víctor VM, Tur R, Alvarez-Barrientos A, Moncada S, Esplugues JV, D'Ocón P (2005) Circ Res 97:1063–1069
14. Chen Z, Zhang J, Stamler JS (2002) Proc Natl Acad Sci USA 99:8306–8311
15. Chen Z, Foster MW, Zhang J, Mao L, Rockman HA, Kawamoto T, Kitagawa K, Nakayama KI, Hess DT, Stamler JS (2005) Proc Natl Acad Sci USA 102:12159–12164
16. Chen Z, Stamler JS (2006) Trends Cardiovasc Med 16:259–265
17. Sydow K, Daiber A, Oelze M, Chen ZQ, August M, Wendt M, Ullrich V, Mulsch A, Schulz E, Keaney JF, Stamler JS, Munzel T (2004) J Clin Invest 113:482–489
18. Munzel T, Hink U, Yigit H, Macharzina R, Harrison R, Mulsch A (1999) Br J Pharmacol 127:1224–1230
19. Munzel T, Sayegh H, Freeman BA, Tarpey MM, Harrison DG (1995) J Clin Invest 95:187–194
20. Gori T, Parker JD (2002) Circulation 106:2404–2407
21. Gori T, Parker JD (2002) Circulation 106:2510–2513
22. Wenzl MV, Beretta M, Gorren ACF, Zeller A, Baral PK, Gruber K, Russwurm M, Koesling D, Schmidt K, Mayer B (2009) J Biol Chem 284:19878–19886
23. Fink B, Dikalov S, Bassenge E (2000) Free Radic Biol Med 28:121–128
24. Dikalov S, Fink B, Skatchkov M, Stalleicken D, Bassenge E (1998) J Pharmacol Exp Ther 286:938–944
25. Laursen JB, Somers M, Kurz S, McCann L, Warnholtz A, Freeman BA, Tarpey M, Fukay T, Harrison DG (2001) Circulation 103:1282–1288
26. Bonini MG, Stadler K, de Silva SO, Corbett J, Dore M, Petranka J, Fernandes DC, Tanaka LY, Duma D, Laurindo FRM, Mason RP (2008) Proc Natl Acad Sci USA 105:8569–8574
27. Thatcher GRJ, Nicolescu AC, Bennett BM, Toader V (2004) Free Radic Biol Med 37:1122–1143
28. PDB ID: 1CW3, Ni L, Zhou J, Hurley TD, Weiner H (1999) Protein Sci 8:2784–2790

29. Zhao Y, Truhlar DG (2008) Theor Chem Account 120:215–241
30. Ditchfield R, Hehre WJ, Pople JA (1971) J Chem Phys 54:724–728
31. Hratchim HP, Schlegel HB (1971) J Chem Phys 120:9918–9924
32. Cioslowsky J (1989) J Am Chem Soc 111:8333–8336
33. Gaussian 09, Revision A.02, M. J. Frisch et al
34. Bode BM, Gordon MS (1998) J Mol Graphics Modell 16:133
35. Schaftenaar G, Noordik JH (2000) J Comput Aided Mol Design 14:123–134
36. Arenas JF, Otero JC, Peláez D, Soto J, Serrano-Andrés L (2004) J Chem Phys 121:4127–4132
37. Arenas JF, Centeno SP, López-Tocón I, Peláez D, Soto J (2003) J Mol Struct (Theochem) 630:17–23
38. Soto J, Arenas JF, Otero JC, Peláez D (2006) J Phys Chem A 110:8221–8226
39. Arenas JF, Avila JF, Otero JC, Peláez D, Soto J (2008) J Phys Chem A 112:249–255
40. Soto J, Peláez D, Otero JC, Avila JF, Arenas JF (2009) Phys Chem Chem Phys 11:2631–2639
41. Cameron DR, Borrajo AMP, Bennett BM, Thatcher GRJ (1995) Can J Chem 73:1627–1638
42. Choi YJ, Lee YS (2004) Bull Korean Chem Soc 25:1657–1660
43. Nenner I, Schulz GJ (1975) J Chem Phys 62:1747–1758
44. Thatcher GRJ, Weldon H (1998) Chem Soc Rev 27:331–337
45. Artz JD, Toader V, Zavorin SI, Bennett BM, Thatcher GRJ (2001) Biochemistry 40:9256–9264
46. Silbey JS, Alberty RA, Bawendi MG (2005) Physical chemistry, 4th edn. Wiley, New York
47. Lide DR (2009–2010) Handbook of chemistry and physics, 90th edn. CRC Press, Boca Raton, 2009